


 Cite this: *Chem. Commun.*, 2022, 58, 11681

 Received 1st July 2022,  
 Accepted 11th August 2022

DOI: 10.1039/d2cc03661d

rsc.li/chemcomm

## A facile route for the recovery of the ligand of zeolitic imidazolate framework ZIF-94/SIM-1†

 Víctor Berned-Samatán,<sup>id</sup><sup>ab</sup> Lidia Martínez-Izquierdo,<sup>id</sup><sup>ab</sup> Elisa Abás,<sup>id</sup><sup>c</sup>  
 Carlos Téllez<sup>id</sup><sup>ab</sup> and Joaquín Coronas<sup>id</sup><sup>\*ab</sup>

**A facile route for the recycling of the organic ligand from ZIF-94/SIM-1 is reported with a recovery yield of  $92.5 \pm 2.8\%$ . The recycled ligand was used for a new ZIF-94 synthesis compared to the one using fresh ligand. ZIF-94 was embedded in Pebax® 1657 mixed matrix membranes for gas separation of CO<sub>2</sub>/N<sub>2</sub> and CO<sub>2</sub>/CH<sub>4</sub> mixtures.**

Metal-organic frameworks (MOFs) have emerged as very promising materials due to their extraordinary properties (*i.e.* ultrahigh porosity, enormous internal surface areas and chemical tunability).<sup>1</sup> These properties make them of interest in many applications such as gas storage, molecular separation membranes, catalysis, drug delivery and biomedical imaging, among others.<sup>2</sup> However, the application of MOFs at a commercial and industrial level will generate a significant amount of waste, since to ensure an optimal performance they should be periodically renewed.

MOFs are composed of metal ions/clusters coordinated with organic linkers. These linkers are usually expensive and as their complexity increases their price also tends to be higher. To this price increase must be added the inflation in energy and transport costs. Hierarchically for the synthesis, the cost of ligands is higher than that of salts and solvents.<sup>3,4</sup> In particular, MOF zeolitic imidazolate framework ZIF-94,<sup>5</sup> first reported under the name of SIM-1,<sup>6,7</sup> is composed of zinc as the metal ion and 4-methyl-5-imidazolecarboxaldehyde (4-m-5-Imca) as the organic linker. This organic linker can be of particular interest for the synthesis of other materials, which may find

application as catalysts,<sup>8</sup> or anti-inflammatory<sup>9</sup> or dinucleating agents,<sup>10</sup> to name a few. ZIF-94 shares the sod type structure with ZIF-8, the first zinc imidazolate reported, synthesized from 2-methylimidazole (2-mIm).<sup>11</sup> In contrast to 2-mIm, ligand 4-m-5-Imca is *ca.* 40 times more expensive (after reviewing the price lists of different suppliers). However, ZIF-94 presents a better performance than ZIF-8 in certain applications such as CO<sub>2</sub> adsorption with a capacity *ca.* 3 times greater.<sup>5</sup> In this context, the recovery of the reactants (*e.g.* the MOF ligand) could be of great interest for both industry and academia, once the MOF has reached its end of life, particularly in the current times of continuous increasing cost and shortage of raw materials. Strategies for recycling/reuse/regeneration and waste treatment of MOFs must be established and some studies show that it is techno-economically feasible for the synthesis of metal nanoparticles and nanocomposites.<sup>3</sup> In addition, the present study completes some of the recent attempts (*e.g.* recycling solvents and reagents from the synthesis or spent mother liquors<sup>12–17</sup> in line with the high environmental impact of organic solvents in the MOF synthesis<sup>18</sup>) to make the synthesis of MOFs more sustainable, none of them dealing with the dissolution of the MOF to purify and reuse its ligand. The reuse of this ligand from discarded ZIF-94/SIM-1 crystals would save an important part of the energy and resources needed to produce new ligand. Besides, as an example of application, the recycled ligand will be used to produce ZIF-94 for gas separation mixed matrix membranes (MMMs) but it could be used for other purposes.

Herein, we report a facile route to recover 4-m-5-Imca (C<sub>5</sub>H<sub>6</sub>N<sub>2</sub>O) from ZIF-94 (Zn(C<sub>5</sub>H<sub>5</sub>N<sub>2</sub>O)<sub>2</sub>) residues (Fig. 1). Briefly, the MOF structure is broken under basic conditions (pH ≈ 14) in a sodium hydroxide aqueous solution at room temperature for 1 h giving rise to a yellowish clear solution. In this solution, the ligand is deprotonated, while the zinc remains dissolved as the complex anion tetrahydroxozincate. The zinc contained in the MOF is removed by precipitation with sodium sulfide (more stable than the complex anion), forming a colloidal dispersion of zinc sulfide, which can be isolated by centrifugation. This solid (white) could be converted, upon

<sup>a</sup> Instituto de Nanociencia y Materiales de Aragón (INMA), CSIC-Universidad de Zaragoza, Zaragoza 50018, Spain. E-mail: coronas@unizar.es

<sup>b</sup> Chemical and Environmental Engineering Department, Universidad de Zaragoza, Zaragoza 50018, Spain

<sup>c</sup> Laser Laboratory, Chemistry & Environment Group, Faculty of Sciences, Department of Analytical Chemistry, University of Zaragoza, Plaza S. Francisco s/n, 50009 Zaragoza, Spain

† Electronic supplementary information (ESI) available: Experimental procedures of support and membrane fabrication, setup for permeation tests and characterization details. See DOI: <https://doi.org/10.1039/d2cc03661d>



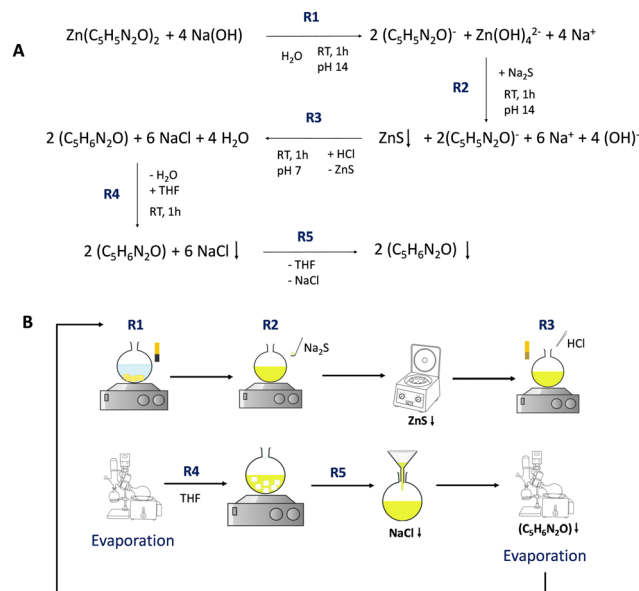


**Fig. 1** Reaction pathway (A) and schematic representation (B) of the recovery of ligand 4-methyl-5-imidazolecarboxaldehyde from ZIF-94 ( $\text{Zn}(\text{C}_5\text{H}_5\text{N}_2\text{O})_2$ ).

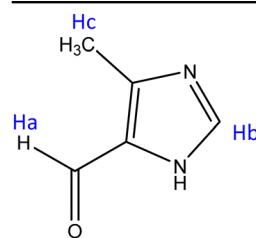
calcination, into zinc oxide for further application. After neutralization of the remaining solution to  $\text{pH} \approx 7$  with hydrochloric acid, water is eliminated with a rotary evaporator obtaining a light yellow solid that is recrystallized in THF to remove the inorganic salts (*i.e.* NaCl). The insoluble precipitate is filtered to obtain a THF solution of the pure 4-m-5-Imca. Finally, THF is eliminated with a rotary evaporator to obtain the solid (light yellow) ligand (4-m-5-Imca-R from now) with a recovery yield of  $92.5 \pm 2.8\%$  (as average of 3 independent experiments).

To confirm the correct recovery of the organic ligand, a series of characterizations (TGA, FTIR, XRD, and NMR) were carried out. Besides, to ensure that the ligand can be reused, a new synthesis of ZIF-94 with the recycled ligand was made to compare its properties with those of the original ZIF-94 synthesized with the as received commercial ligand.<sup>19</sup> The synthesis of both ZIF-94 MOFs, the original and the one with the recycled ligand, was carried out as follows: 7.2 mmol of zinc acetate and 14.4 mmol of sodium hydroxide are dissolved in 6 mL of methanol. Separately, 14.4 mmol of 4-m-5-Imca-R was dissolved in 15 mL of THF. Next, the metal solution was added to the ligand solution and kept under vigorous stirring for 16 h at room temperature. The final product was collected by centrifugation and washed with fresh methanol three times. Afterwards, the ZIF-94 particles were activated by refluxing in 50 mL of methanol for 1.5 h. The resulting ZIF-94 was dried overnight at room temperature with yields of 69–72% for the original and recycled ligand. As shown below, the same characterization techniques applied to the ligand as well as the calculation of the BET specific surface area (SSA) and SEM observation allowed the study of the synthesis of both ZIF-94 materials.

To evaluate the success of the recycling process,  $^1\text{H-NMR}$  studies were conducted on the recovered ligand. According to

**Table 1**  $^1\text{H-NMR}$  signals (ppm) for both 4-m-5-Imca ligands in deuterium oxide

	Commercial	Recovered
Hc	9.65 (s, 1H)	9.66 (s, 1H)
Hb	7.75 (s, 1H)	7.76 (s, 1H)
Hc	2.48 (s, 3H)	2.49 (s, 3H)



the great solubility of the imidazole ligand in water, deuterium oxide was selected as solvent. As seen in Fig. S1 (ESI<sup>†</sup>), all  $^1\text{H}$  signals are practically the same for the recovered imidazole ligand and the as-received commercial one. The corresponding assignment, confirmed by  $^1\text{H-}^{13}\text{C}$  HSCQ (Fig. S2, ESI<sup>†</sup>), is shown in Table 1. It is worth mentioning that in case the imidazole was still linked to the metallic center all signals would experience a low-field shift.<sup>20</sup> The perfect match between the spectrum of the commercial imidazole and the recovered one is consistent with the great efficacy of the recovery process. Moreover, since no additional signals were evidenced, it can be concluded that this new synthetic procedure is efficient and clean.

TGA studies in air (Fig. S3, ESI<sup>†</sup>) showed the same degradation curve from 155 to 250 °C for the recycled 4-m-5-Imca and the commercial one. Both ZIF-94 syntheses also showed the same degradation curves with residues of 30 wt% generated from the inorganic part of the MOF converted to zinc oxide.

XRD diffractograms (Fig. 2A)<sup>21,22</sup> show the same peaks for the ligands proving the high purity of the 4-m-5-Imca-R. The XRD of both synthesized ZIFs are identical corroborating that the recycled ligand can be efficiently reused.

The FTIR-ATR spectra of ZIFs and ligands are depicted in Fig. 2B, revealing similar spectra, with the main bands at

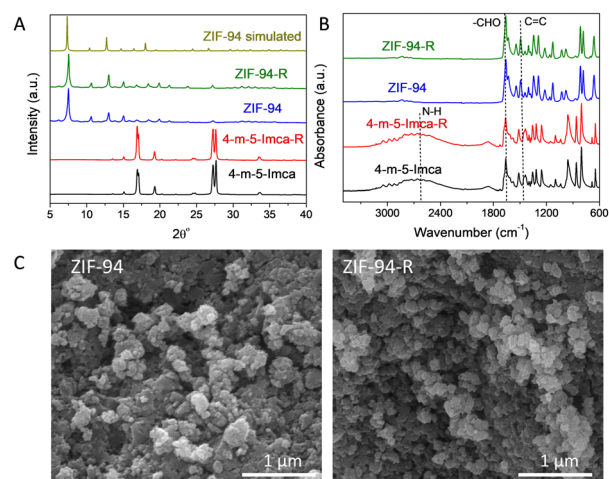


**Fig. 2** XRD patterns (A) and FTIR-ATR spectra (B) of ligands and ZIFs. SEM images (C) of both ZIFs.



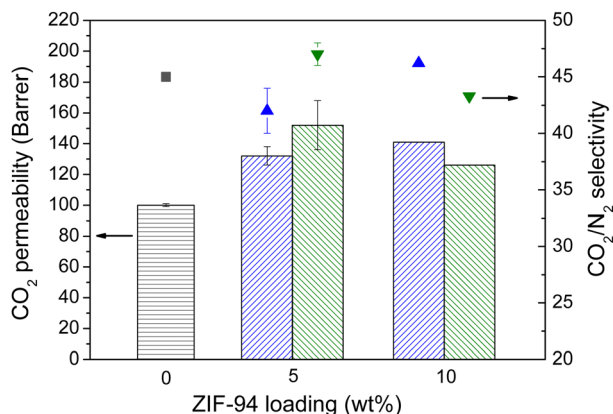


Fig. 3 Gas separation performance at 35 °C and 3 bar feed pressure for the MMMs prepared with ZIF-94 (blue) and ZIF-94-R (green) compared with the bare polymer (grey) for 15/85 CO<sub>2</sub>/N<sub>2</sub> mixture. Error bars come from the test of three different membranes.

1660 cm<sup>-1</sup>, which correspond to the aldehyde group (-CHO), 1496 cm<sup>-1</sup> and the C=C bond, while, only for the ligand, a broad band centered at 2500 cm<sup>-1</sup> is related to the N-H.<sup>23</sup>

Nitrogen adsorption isotherms (Fig. S4A, ESI<sup>†</sup>) are practically the same for both ZIFs, corresponding to BET SSA values of 545 m<sup>2</sup> g<sup>-1</sup> and 534 m<sup>2</sup> g<sup>-1</sup> for ZIF-94 produced from fresh and recycled imidazole, respectively. In addition, they exhibit identical type I adsorption curves with a pronounced increase in adsorption at values approaching  $p/p^\circ = 1$ , which is due to capillary condensation between the ZIF nanoparticles, being in accordance with the literature.<sup>24</sup> In addition, Fig. S4B (ESI<sup>†</sup>) shows the CO<sub>2</sub> adsorption isotherms at 294 K with similar behavior and adsorption capacities of 2.2 mmol g<sup>-1</sup> at 100 kPa for both fresh and recycled ZIF-94. This value is in agreement with previously reported results.<sup>25</sup> Fig. 2C depicts SEM images of both ZIFs with similar particle size of *ca.* 60 ± 10 nm and 58 ± 12 nm, respectively.

To further confirm the correct reutilization of the recycled ligand, Pebax<sup>®</sup> 1657 MMMs were prepared with both ZIF-94 and ZIF-94-R. Pebax type copolymers, and in particular the one chosen here, are considered as very effective membrane materials for CO<sub>2</sub> separation.<sup>26</sup> The membranes were prepared using a modified reported method.<sup>25</sup> Concisely, 0.3 g of the polymer was dissolved in 6.7 g of 70 : 30 EtOH : H<sub>2</sub>O mixture under reflux for 1 h. Afterwards, the polymer solution was added to a previously prepared dispersion with the appropriated amount of the ZIF (5 and 10 wt%) in 3 g of the EtOH : H<sub>2</sub>O solution. This mixture was subjected to several sonication and stirring cycles until achieving a homogenous suspension. Finally, the suspension was cast into a glass Petri dish and dried at room temperature for 48 h.

Due to the CO<sub>2</sub>-philic character of ZIF-94,<sup>5</sup> the MMMs were tested in gas separation experiments of CO<sub>2</sub>/N<sub>2</sub> and CO<sub>2</sub>/CH<sub>4</sub> mixtures as explained in the ESI<sup>†</sup>. As depicted in Fig. 3, the MMMs prepared with both, ZIF-94 and ZIF-94-R exhibited a similar CO<sub>2</sub>/N<sub>2</sub> separation performance. Moreover, at 5 wt% of loading, the CO<sub>2</sub> permeability increased for both ZIFs, from 100

Barrer in the bare Pebax<sup>®</sup> 1657 to 132 and 152 Barrer for the original and recovered ZIF-94 MMMs, respectively. This 5 wt% loading is the maximum amount of ZIF that can be incorporated into the Pebax<sup>®</sup> 1657 matrix without affecting the separation performance. Higher concentrations of ZIF in the MMMs implied a decrease in the CO<sub>2</sub> permeability, which is related to the agglomeration of the ZIF particles inside the polymer matrix. Particularly, the membrane prepared with 10 wt% of the original ZIF-94 exhibited higher CO<sub>2</sub> permeability in CO<sub>2</sub>/N<sub>2</sub> separation mixtures, although the difference was not large enough to consider this loading as optimum. Analogous results but with lower selectivity values were achieved when applied the membranes to the CO<sub>2</sub>/CH<sub>4</sub> mixture (see Fig. S5, ESI<sup>†</sup>). These results are in concordance with the time-lag experiments shown in Fig. S6 (ESI<sup>†</sup>), where the similar CO<sub>2</sub> solubility values of 150–160 cm<sup>3</sup>(STP) cm<sup>-3</sup> cmHg<sup>-1</sup> for both MMMs (with 5 wt% of fresh and recycled ZIF-94), superior to that of the bare polymer (130 cm<sup>3</sup>(STP) cm<sup>-3</sup> cmHg<sup>-1</sup>), agree with the similar CO<sub>2</sub> adsorption capacities seen above.

In summary, 4-m-5-Imca was successfully recovered from ZIF-94 with a yield of 92.5 ± 2.8% and high purity as confirmed by TGA, FTIR, XRD, and NMR techniques. Furthermore, as a model to show the efficiency of the ligand reuse, ZIF-94 crystals prepared with the recovered and the commercial ligands were incorporated into Pebax<sup>®</sup> 1657 MMMs reaching the highest separation performance at 5 wt% MOF loading. These results encourage us to believe that this methodology can be extrapolated to other MOF ligands, making more sustainable their future application.

Financial support from the Spanish research project PID2019-104009RB-I00/AEI/10.13039/501100011033 and the Aragón Government (T43\_20R) are gratefully acknowledged. V. B.-S. Thanks the Spanish MINECO for the predoctoral grant BES-2017-080209 awarded. L. M.-I. Thanks the Aragón Government for her PhD grant. The authors would like to acknowledge the use of the Servicio General de Apoyo a la Investigación-SAI and the use of instrumentation as well as the technical advice provided by the National Facility ELECOMI ICTS, node "Laboratorio de Microscopias Avanzadas" at the University of Zaragoza. Dr Javier Lasobras is thanked for the carbon dioxide adsorption studies.

## Conflicts of interest

There are no conflicts to declare.

## Notes and references

- H.-C. Zhou, J. R. Long and O. M. Yaghi, *Chem. Rev.*, 2012, **112**, 673–674.
- R. Freund, O. Zaremba, G. Arnauts, R. Ameloot, G. Skorupskii, M. Dincă, A. Bavykina, J. Gascon, A. Ejsmont, J. Goscińska, M. Kalmutzki, U. Lächelt, E. Ploetz, C. S. Diercks and S. Wuttke, *Angew. Chem., Int. Ed.*, 2021, **60**, 23975–24001.
- P. Kumar, B. Anand, Y. F. Tsang, K. H. Kim, S. Khullar and B. Wang, *Environ. Res.*, 2019, **176**, 108488.
- D. DeSantis, J. A. Mason, B. D. James, C. Houchins, J. R. Long and M. Veenstra, *Energy Fuels*, 2017, **31**, 2024–2032.



- 5 W. Morris, N. He, K. G. Ray, P. Klonowski, H. Furukawa, I. N. Daniels, Y. A. Houndonougbo, M. Asta, O. M. Yaghi and B. B. Laird, *J. Phys. Chem. C*, 2012, **116**, 24084–24090.
- 6 S. Aguado, J. Canivet and D. Farrusseng, *Chem. Commun.*, 2010, **46**, 7999–8001.
- 7 M. Baias, A. Lesage, S. Aguado, J. Canivet, V. Moizan-Basle, N. Audebrand, D. Farrusseng and L. Emsley, *Angew. Chem., Int. Ed.*, 2015, **54**, 5971–5976.
- 8 L. S. Long, X. M. Chen, X. L. Yu, Z. Y. Zhou and L. N. Ji, *Polyhedron*, 1999, **18**, 1927–1933.
- 9 M. Nath, P. K. Saini and A. Kumar, *J. Organomet. Chem.*, 2010, **695**, 1353–1362.
- 10 C. T. Brewer, G. Brewer, M. Shang, W. R. Scheidt and I. Muller, *Inorg. Chim. Acta*, 1998, **278**, 197–201.
- 11 K. S. Park, Z. Ni, A. P. Cote, J. Y. Choi, R. Huang, F. J. Uribe-Romo, H. K. Chae, M. O’Keeffe and O. M. Yaghi, *Proc. Natl. Acad. Sci. U. S. A.*, 2006, **103**, 10186–10191.
- 12 N. Jamil, N. H. Alias, M. Z. Shahrudin and N. H. Othman, *Key Eng. Mater.*, 2019, **797**, 48–54.
- 13 M. R. Hasan, L. Paseta, M. Malankowska, C. Téllez and J. Coronas, *Adv. Sustainable Syst.*, 2022, **6**, 2100317.
- 14 S. Gökpınar, T. Diment and C. Janiak, *Dalton Trans.*, 2017, **46**, 9895–9900.
- 15 M. García-Palacín, J. I. Martínez, L. Paseta, A. Deacon, T. Johnson, M. Malankowska, C. Téllez and J. Coronas, *ACS Sustainable Chem. Eng.*, 2020, **8**, 2973–2980.
- 16 F. Şahin, B. Topuz and H. Kalıpcılar, *Microporous Mesoporous Mater.*, 2018, **261**, 259–267.
- 17 M. Zhang, Z. Yu, Z. Sun, A. Wang, J. Zhang, Y. Y. Liu and Y. Wang, *Microporous Mesoporous Mater.*, 2021, **327**, 111423.
- 18 V. Ntoulos, I. Kousis, D. Papadaki, A. L. Pisello and M. N. Assimakopoulos, *Energies*, 2021, **14**, 1–22.
- 19 D. Madhav, M. Malankowska and J. Coronas, *New J. Chem.*, 2020, **44**, 20449–20457.
- 20 B. Barszcz, S. A. Hodorowicz, K. Stadnicka and A. Jabłońska-Wawrzycka, *Polyhedron*, 2005, **24**, 627–637.
- 21 Mercury – The Cambridge Crystallographic Data Centre (CCDC), <https://www.ccdc.cam.ac.uk/solutions/csd-system/components/mercury/>.
- 22 Structures, <https://www.ccdc.cam.ac.uk/structures/Search?Compound=ZIF-8&DatabaseToSearch=Published>.
- 23 F. Cacho-Bailo, M. Etxeberria-Benavides, O. Karvan, C. Téllez and J. Coronas, *CrystEngComm*, 2017, **19**, 1545–1554.
- 24 J. Sánchez-Lainez, B. Zornoza, A. F. Orsi, M. M. Łozińska, D. M. Dawson, S. E. Ashbrook, S. M. Francis, P. A. Wright, V. Benoit, P. L. Llewellyn, C. Téllez and J. Coronas, *Chem. – Eur. J.*, 2018, **24**, 11211–11219.
- 25 A. Sabetghadam, X. Liu, M. Benzaqui, E. Gkaniatsou, A. Orsi, M. M. Łozińska, C. Sicard, T. Johnson, N. Steunou, P. A. Wright, C. Serre, J. Gascon and F. Kapteijn, *Chem. – Eur. J.*, 2018, **24**, 7949–7956.
- 26 M. Malankowska, J. Coronas, A. S. Embaye, L. Martínez-Izquierdo and C. Téllez, *Energy Fuels*, 2021, **35**, 17085–17102.

